Theoretical assessment of the elastic constants and hydrogen storage capacity of some metal-organic framework materials

Amit Samanta
Department of Materials Science and Engineering, Ohio State University, Columbus, Ohio 43210

Terumi Furuta
Honda R&D Co., Ltd., Wako Research Center, 1-4-1 Chuo Wako, Saitama 351-0193, Japan

Ju Li[a)]
Department of Materials Science and Engineering, Ohio State University, Columbus, Ohio 43210

(Received 25 January 2006; accepted 20 July 2006; published online 25 August 2006)

Metal-organic frameworks (MOFs) are promising materials for applications such as separation, catalysis, and gas storage. A key indicator of their structural stability is the shear modulus. By density functional theory calculations in a 106-atom supercell, under the local density approximation, we find $c_{11}=29.2$ GPa and $c_{12}=13.1$ GPa for Zn-based MOF 5. However, we find c_{44} of MOF-5 to be exceedingly small, only 1.4 GPa at $T=0$ K. The binding energy E_{ads} of a single hydrogen molecule in MOF-5 is evaluated using the same setup. We find it to be -0.069 to -0.086 eV/H_2 near the benzene linker and -0.106 to -0.160 eV/H_2 near the Zn_4O tetrahedra. Substitutions of chlorine and hydroxyl in the benzene linker have negligible effect on the physisorption energies. Pentacoordinated copper (and aluminum) in a framework structure similar to MOF-2 gives $E_{ads}\approx -0.291$ eV/H_2 (and -0.230 eV/H_2), and substitution of nitrogen in benzene (pyrazine) further enhances E_{ads} near the organic linker to -0.16 eV/H_2, according to density functional theory with local density approximation. © *2006 American Institute of Physics*.
[DOI: 10.1063/1.2337287]

I. INTRODUCTION

The rational synthesis of open-framework hybrid compounds, especially those employing rigid organic linkers such as carboxylate, bipyridyl, and other multifunctional ligands, has attracted much attention recently.[1–5] Metal-organic framework (MOF) is a class of highly crystalline materials with metal oxide cores and organic ligand linkers, which recently broke the world record in specific surface area.[6] The nanoporous MOFs are simple and cheap to produce in bulk quantities, with tunable pore size and organic functionalities. Thus they may find use in a wide range of industrial applications such as separation, catalysis, and gas storage. Our interest in MOFs mainly stems from their potential use as physisorption medium for hydrogen storage.

Hydrogen storage for fuel-cell vehicles is under intensive research[7–10] because of the ever-growing concerns over the environmental impact and availability of fossil fuels. Various schemes for storing hydrogen including gas, liquid, and solid-state storage are proposed. Current methods for on-board storage are unsatisfactory due to real and perceived dangers of high-pressure tank and problems of maintaining hydrogen in liquid form. The hydrogen storage material for automotive use must be mechanically stable near the temperatures and pressures of operation, should be cheaply synthesizable, and be able to uptake and desorb hydrogen in a short time. Depending on the nature of bonding, there are two ways by which hydrogen can be stored—chemisorption and physisorption. On the chemisorption side, metal hydrides such as $LiAlH_4$ which can store >10 wt % hydrogen have been developed,[11] but the drawbacks are unfavorable kinetics, reusability, and thermal management issues. On the physisorption side, much attention has been focused on carbon nanostructures,[12] but it has been rather conclusively demonstrated that much of the early optimisms are misguided.[13–15] Lately, there have been studies of H_2 physisorption by ceramic (e.g., BN) nanotubes[16] and metal-loaded zeolites (Zn-exchange zeolites, *A*, *X*, and *Y* zeolites, etc).[17,18] We note that employing nanostructures synthesized with high energy input and high cost for gas storage does not make environmental or economic sense. Cheap, low-energy synthesis of stable nanoporous material is critical for the success of the H_2 physisorption paradigm.

The chemical formula of MOF-5 (Ref. 19) is $(OZn_4(BDC)_3)_n$, where BDC stands for 1,4-benzenedicarboxylate $[O_2C-C_6H_4-CO_2]^{2-}$. Six BDCs connect to one $[OZn_4]^{6+}$ core, and one may call the octahedron formed by the six outlying C vertices the secondary building unit (SBU), $[OZn_4(O_2C)_6]^{6+}$. The MOF-5 lattice is then formed by linking the SBUs with $-C_6H_4-$. Each SBU can also be regarded as four ZnO_4 tetrahedra sharing a common O center and connecting to six C vertex atoms. MOF-5 has space group $Fm\bar{3}m$, and as shown in Fig. 1 it actually consists of SBUs of two different orientations A and B, arranged similar to the NaCl lattice. The smallest periodic cell one can study is then $(OZn_4(BDC)_3)_2$ with 106 atoms and molecular

[a)]Author to whom correspondence should be addressed. Electronic mail: li.562@osu.edu

 © 2006 American Institute of Physics

Downloaded 01 Sep 2006 to 164.107.79.177. Redistribution subject to AIP license or copyright, see http://jcp.aip.org/jcp/copyright.jsp

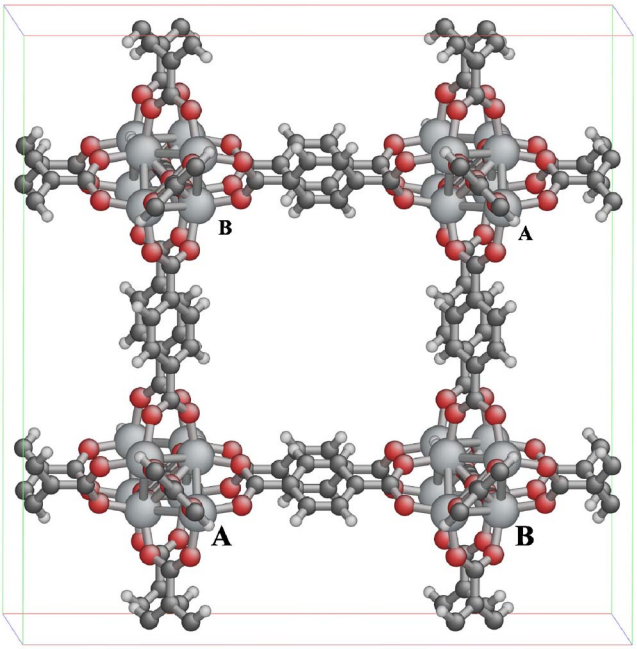

FIG. 1. Atomic structure (O, red; C, black; H, white) of MOF-5. Two different SBU orientations A and B can be distinguished.

weight of 1540 Da, consisting of one SBU of each orientation. The $-C_6H_4-$ linkers running in the [100] direction have two orientations as well, 90° to each other.

Experimental measurements of MOF's physical properties such as elastic constants are scarce at the moment. Here we report first-principles calculations of the elastic constants and electronic structure of MOF-5 using plane wave density functional theory[20] (DFT) with local density approximation (LDA),[21,22] followed by H_2 physisorption energy calculations.[13] Experiments performed by Rowsell *et al.* show that MOF-5 can adsorb up to 1.3 wt % hydrogen at 77 K and 1 atm H_2 partial pressure.[23] In parallel a large number of theoretical calculations have been carried out[24–30] for MOF-5. We use these existing results to benchmark our calculations and identify some basic building units which may have higher H_2 adsorption energies. These are then used to design chemically sensible structures which are predicted to have higher H_2 uptake at room temperature. The calculations, within the limitations of DFT-LDA, indicate that framework structures similar to MOF-2, which we name P-1 to P-3, with pentacoordinated copper and aluminum and pyrazine ($-C_6H_2N_2-$) linkers, have significantly stronger affinity for H_2 compared to Zn-based MOF-5.

Here we must caution that LDA cannot be expected to give accurate values of weak dispersive (van der Waals) forces, especially long-ranged interactions between two electron clouds with negligible overlap, since the long-ranged attraction ($\propto R^{-6}$) originates from vacuum-mediated correlated dipole-dipole (polarization) fluctuations. However, compared with other pure density functionals such as PW91 (Ref. 31) and PBE (Ref. 32) that involve similar computational costs, LDA does give better results[33] for extended systems when the interaction range is intermediate. For example, LDA predicts the graphite interplanar spacing to be 3.3 Å (experiment, 3.35 Å; PW91, >3.8 Å) and binding energy 20 meV/atom (experiment, 35±10 meV/atom; PW91, 5 meV/atom).[34] PW91 predicts purely repulsive interactions between H_2—graphite and single walled carbon nanotube,[35] while LDA gives binding energies that are at least on the same scale as experimental estimates,[36–38] even though it tends to be overbinding by a factor of ~2. Also, in this case the dependence of LDA binding energy on distance is in reasonable agreement with the second-order Møller-Plesset perturbation theory.[33,39] While it has been noted that this moderate success is due to fortuitous cancellation of errors,[40,41] from a practical standpoint LDA does seem to be a safer choice when plane wave DFT code is used. In the case of H_2—MOF-5 interactions, recent PBE calculation[27] gives ~10 meV/H_2 adsorption energy near benzene linker and ~20 meV/H_2 near oxide core in the low-coverage limit. This is clearly underbinding, since experimental estimate for the adsorption enthalpy in MOF-5 exceeds 40 meV/H_2 even at high coverages.[42] On the other hand, LDA results (69–86 meV/H_2 near linker and 106–160 meV/H_2 near oxide[30]) seem to be overbinding compared to high-level quantum chemistry calculations on MOF-5 fragments (43 meV/H_2 near linker[25] and 71 meV/H_2 near oxide[24]), again somewhat consistent by a factor of ~2. We note that the main purpose of the present work is not to get accurate adsorption energy values for MOF-5, for which high-quality measurements[42] and calculations[24,25] are already available, but to scope out possible new framework structures with sorption energies far exceeding those of MOF-5. Therefore relative comparison of sorption energies within DFT-LDA might be much more meaningful than the absolute values obtained. Also, we expect that as the adsorption energy gets larger due to charge-transfer and polar interactions in addition to the weak dispersive interactions, the relative accuracy of LDA result will improve.

II. CALCULATION METHOD AND RESULTS FOR MOF-5

A feasible theoretical approach to studying H_2 uptake is to calculate the H_2 adsorption free energy $\Delta\mu=\Delta h-T\Delta s$ in a given material, where Δh is the change in specific enthalpy and Δs the change in specific entropy of a hydrogen molecule before and after adsorption. Assuming that the entropy of hydrogen in adsorbed state is far less than that of the gaseous state at 1 atm, for near room temperature adsorption/desorption to occur, Δh should be $\sim 10k_BT$ per molecule[13,14,43] or ~200 meV/H_2. In addition to finding high-adsorption energy sites in our DFT calculations, we also need to determine the abundance of such sites in order to meet the storage capacity requirement.

We use the projector augmented-wave[44] (PAW) method as implemented in the Vienna *ab initio* simulation package (VASP).[45,46] The wave functions are expanded in plane waves up to a kinetic energy cutoff of 520 eV. The special **k**-point scheme of Monkhorst and Pack[47] is used with $1\times1\times1$ and $2\times2\times2$ meshes for Brillouin zone integration for the 106-atom oblique supercell (plus H_2 molecules). The results are essentially identical for the two **k**-point meshes. Electronic relaxation stops when the total energy difference between two consecutive iterations is less than 10^{-5} eV. To determine

Downloaded 01 Sep 2006 to 164.107.79.177. Redistribution subject to AIP license or copyright, see http://jcp.aip.org/jcp/copyright.jsp

TABLE I. Comparison of the calculated and experimental (Ref. 19) equilibrium structures of MOF-5.

	Expt.	Calc.
	Bond length	
Zn–Zn	3.16 Å	3.14 Å
Zn–O	1.91 Å	1.92 Å
O–C	1.30 Å	1.27 Å
	Bond angle	
O–C–O	125.0°	125.8°
O–C–C	117.5°	117.0°
Zn–O–C	130.4°	130.5°
Zn–Zn–Zn	60.0°	60.0°

the local energy minimum for a given configuration we relax the ions using the conjugate gradient algorithm,[48] which stops when the energy difference between two consecutive steps is less than 10^{-4} eV. The equilibrium lattice constant of MOF-5 is calculated to be $a_0=25.637$ Å, in good agreement with the experimental value of 25.669 Å.[19] Table I shows comparison of the relaxed structure with the reported structure from x-ray diffraction.[19]

A. Physical properties

Rational design of MOF (Refs. 49 and 50) requires mechanistic understanding of the framework stability. One possible reason that an evacuated framework becomes unstable at room temperature is due to elastic instability.[51,52] Using VASP, we calculate the bulk modulus B of MOF-5 to be 18.5 GPa by fitting the energy-volume data to a cubic polynomial. With a second, tetragonal deformation mode, we find that $c_{11}=29.2$ GPa and $c_{12}=13.1$ GPa. However, we find c_{44} to be exceedingly small, only 1.4 GPa, with an xy shear energy-strain calculation, with all the internal degrees of freedom fully relaxed. Therefore, shear strain of xy (and yz and xz) nature seems to be the most vulnerable deformation mode for the MOF-5 structure. It would be a good idea to deconvolute these elastic constants in terms of the elementary properties of the SBUs and linkers, whose combinations present nearly infinite possibilities. In other words, one ideally would like to predict the finite-T elastic constants of any framework design before its synthesis is attempted in the laboratory, to ensure that the elastic constant tensor is positive definite[51,52] at the intended temperature, so the framework is synthesizable. To accomplish this, we first assume that the BDC is infinitely rigid, connected by a Hookean spring network resembling the soft organic linkers. We perform a separate calculation by stretching one BDC linker and obtained a spring constant of $k_s=62.8$ N/m. Using the formula $B=2k_s/3a_0$ for cubic framework, we find $B\approx 16.7$ GPa, which agrees well with the actual framework result. On the other hand, the shear modulus is zero for a cubic spring network. A simple Keating model[53] may be used to account for the small but finite c_{44}, which is due to "bond-angle" dependence near the metal core. If we phenomenologically assume that two BDC linkers connected to the same metal core with $\pi/2$ angle at equilibrium sustain energy penalty $\Delta E=k_\theta(\theta-\pi/2)^2/2$ for any other angle θ, then there are

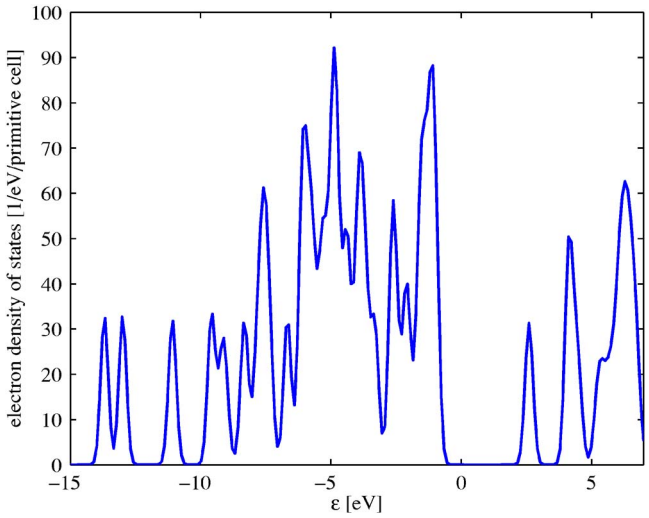

FIG. 2. Calculated electron density of states of MOF-5.

12 such pairs at a metal core, and the corresponding $c_{44}=32k_\theta/a_0^3$ at $T=0$ K. This allows us to extract $k_\theta\approx 4.9$ eV from the VASP result. k_s and k_θ may then be used in future finite-temperature molecular dynamics (MD) simulations. It is well known[51] that c_{44} tends to decrease with T and may vanish at some critical T.

Since benzene can undergo electrophilic substitutions, simulations are also performed in MOF-5-like structures with linkers such as 3-chloro-1,4-benzenedicarboxylate $[O_2C-C_6H_3Cl-CO_2]^{2-}$ [similar to the Br–BDC linker in MOF-111 (Ref. 54)] and 3-hydroxy-1,4-benzenedicarboxylate $[O_2C-C_6H_3OH-CO_2]^{2-}$, framework structures which we shorthand as Cl-MOF-5 and OH-MOF-5, respectively. A small dihedral angle of $\Theta=5.5°$ between the benzene plane and carboxylate (paddle wheel) has been reported for the BDC linkers in MOF-2,[55] due to steric repulsion between the hydrogen atoms, which is verified by us in DFT calculations. On the other hand, Θ in MOF-5 has been reported to be zero.[19] We find that MOF-5, Cl-MOF-5, and OH-MOF-5 all have zero Θ at equilibrium. Relaxations following perturbing the benzene ring by 3° and 90° from its equilibrium position and *ab initio* MD calculations performed at 300 K do not show any paddle-wheel behavior in these structures.

The calculated electronic density of states (DOS) for MOF-5 is shown in Fig. 2, with a band gap of 2.7 eV. Bordiga *et al.* reported a band gap of 3.5 eV (350 nm) for MOF-5 with ultraviolet-visible (UV-vis) diffuse reflectance spectrometry,[56] corresponding to ligand-to-metal charge-transfer transition. Since LDA systematically underestimates the band gap, our result is within reason. We expect that Fig. 2 would be quite accurate after a "scissor" operation.[57]

B. Hydrogen adsorption

In the next step, H_2 adsorption energies at different sites in MOF-5, Cl-MOF-5, and OH-MOF-5 are calculated. From the analysis of inelastic neutron scattering spectra,[30,58] it was suggested that there are two sites for H_2 adsorption: (1) Zn_4O_{13} cluster and (2) near benzene. We place H_2 molecules

Downloaded 01 Sep 2006 to 164.107.79.177. Redistribution subject to AIP license or copyright, see http://jcp.aip.org/jcp/copyright.jsp

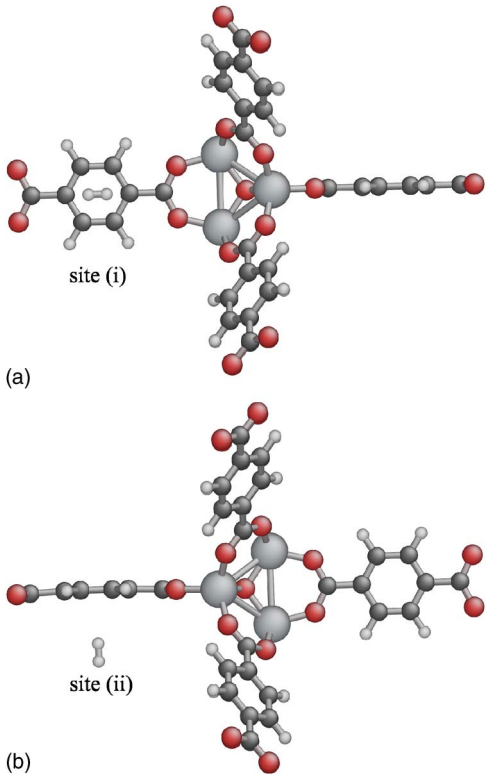

FIG. 3. Equilibrium configurations of hydrogen adsorbed near benzene in MOF-5. (a) H_2 parallel to benzene plane and parallel to BDC axis (at 2.3 Å from benzene center). (b) H_2 oriented perpendicular to benzene plane (center of H_2 at 2.7 Å from benzene center).

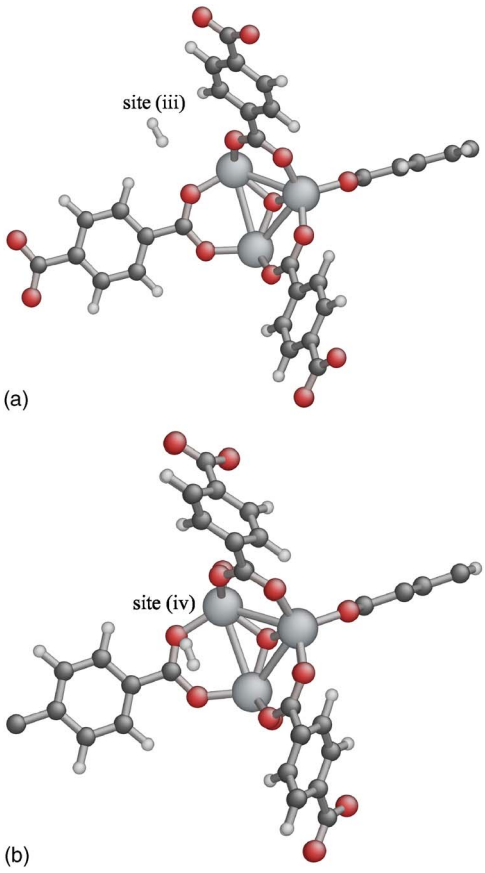

FIG. 4. Equilibrium configurations of hydrogen adsorbed near metal oxide in MOF-5. (a) H_2 placed near oxygen of BDC (center of H_2 at 2.7 Å from benzene center). (b) H_2 parallel to oxygen atoms of one of the six BDCs originating from a Zn_4O (center of H_2 at 2.3 Å from benzene center).

of different orientations in the proximity of various sites and obtain the fully relaxed structures (both H_2 and MOF): (i) H_2 parallel to the plane of benzene and parallel to the BDC running axis [Fig. 3(a)], (ii) H_2 perpendicular to the plane of benzene [Fig. 3(b)], (iii) H_2 near oxygen of BDC and away from Zn_4O cluster [Fig. 4(a)], and (iv) H_2 parallel to oxygen atoms of BDC [Fig. 4(b)].

With the fully optimized structures, the adsorption energy E_{ads} is computed as $E_{ads}=E_{MOF\text{-}5+H_2}-(E_{MOF\text{-}5}+E_{H_2})$, where $E_{MOF\text{-}5+H_2}$ is the energy of hydrogen adsorbed in MOF-5 while $E_{MOF\text{-}5}$ and E_{H_2} correspond to the energies of pure MOF-5 and H_2, respectively. Due to the very small magnitude of E_{ads}, care is taken to adopt exactly the same supercell, energy cutoff, **k**-point sampling, etc., in calculating $E_{MOF\text{-}5+H_2}$, $E_{MOF\text{-}5}$, and E_{H_2} to ensure maximum error cancellation. Because hydrogen is very light, the zero-point vibrational energy $h\nu/2$ is significant (272 meV for free H_2 molecule). However, Williams *et al.* measured the Raman spectra of H_2 in free and adsorbed states in carbon nanotubes[59] and found the shifts of the H–H stretch frequency to be on the order of 1 cm^{-1}, which corresponds to ~0.1 meV. This contribution can therefore be safely neglected. On the other hand, the center-of-mass zero-point vibrations of physisorbed H_2 molecule could give non-negligible contributions to Δh, in the direction of *reducing* the thermodynamic preference of the physisorbed state compared to the bare E_{ads}. An exact calculation is complex because the framework vibrational frequencies are changed by the physisorption as well, although the changes would not be as significant as that of H_2 itself, due to the more massive atoms in the framework and also preexisting spring constants. A rough but simple estimate is then the following. We assume that the framework is rigid, and the H_2 trapping potential takes the form $E\approx E_{ads}(1-|\mathbf{x}-\mathbf{x}_0|^2/\Delta^2)$, where Δ is the effective trapping range of the potential and $\mathbf{x}$ is the center of mass of the molecule. A reasonable estimate from our calculations is $\Delta=1$ Å. The oscillator frequency is then $\nu=(k/m_{H_2})^{1/2}/2\pi=(-2E_{ads}/\Delta^2 m_{H_2})^{1/2}/2\pi\propto|E_{ads}|^{1/2}$. Assuming $E_{ads}=-100$ meV, we then get $\nu\approx 5$ THz and the zero-point energy $E_{zero\text{-}pt}=3h\nu/2\approx 30$ meV, which is a significant fraction of E_{ads}. Also note the square root dependence ($\propto|E_{ads}|^{1/2}$) of this contribution, which means that it becomes relatively more important as $|E_{ads}|$ gets smaller. In this paper we calculate E_{ads} only, and not $\Delta h\equiv E_{ads}+E_{zero\text{-}pt}$ due to the complexity of computing $E_{zero\text{-}pt}$, which is not entirely necessary in the initial screening process. But the above point needs to be kept in mind in accessing the thermodynamic stability of physisorption.

We have found physisorption sites in MOF-5 (Table II) near both the benzene linker ($E_{ads}=-0.069$ to -0.086 eV) and metal oxide core ($E_{ads}=-0.106$ to -0.160 eV). This confirms previous theoretical[24,25,27,28] and experimental[30] propositions that the metal oxide cores offer more attractive H_2 sorption sites. For sites near benzene, E_{ads} is minimized at

Downloaded 01 Sep 2006 to 164.107.79.177. Redistribution subject to AIP license or copyright, see http://jcp.aip.org/jcp/copyright.jsp

TABLE II. Calculated E_{ads} for H_2 in MOF-5 (Figs. 3 and 4). The zero-point vibrational energies have been ignored.

Position of H_2		E_{ads} (eV/H_2)
Near benzene	Site (i): parallel to benzene plane	−0.069
	Site (ii): perpendicular to benzene plane	−0.086
Near Zn cluster	Site (iii): away from Zn_4O	−0.106
	Site (iv): parallel to oxygen of BDC	−0.160

the center of benzene ring for H_2 of the perpendicular orientation [E_{ads}=−0.086 eV/H_2, nearest C from H_2 center is 3.05 Å, Fig. 3(b)].

We perform similar calculations for Cl-MOF-5 and OH-MOF-5. The charge isosurface plots show considerable amount of electron concentration around the substituted Cl and O (of hydroxyl) groups. However, calculations with H_2 molecules initially placed near Cl or oxygen of OH have final equilibrium position at site (iii) or (iv) and do not yield any new adsorption site, nor is E_{ads} changed significantly. For example, although after Cl substitution the H_2 molecule moves adjacent to both Cl and O, we still get E_{ads}= −0.104 eV/H_2, which is almost identical to E_{ads}= −0.106 eV/H_2 without the Cl substitution. Relaxed structure of MOF-5 with four H_2 molecules placed parallel to the BDC axis, two above and two below the benzene plane, has E_{ads} ~−0.05 eV/H_2 and equilibrium separation of ~4.5 Å between them. This suggests significant H_2–H_2 repulsion effect.

Yildirim and Hartman predicted up to 11 wt % H_2 uptake in MOF-5, which is 46 H_2 molecules per $[OZn_4]^{6+}$ core or 92 H_2 per unit cell. Calculations by Mulder *et al.*[28] with 23 H_2 molecules per MOF-5 unit cell also point to the high H_2 uptake by MOF-5 at low temperatures. Comparing with high-level quantum chemistry calculations for MOF-5 fragments by Sagara *et al.*,[24] our values for E_{ads} are higher by ~50%, which should be attributed to the intrinsic error of LDA. Mulder *et al.* have argued that steric hindrance from H_2 molecules already present in neighboring sites results in a decrease in the actual occupancies of H_2 molecules in MOF-5. An increase in the values of E_{ads} would help H_2 to adhere to these open-framework structures till somewhat higher temperatures. With this goal in mind, we explore ways to enhance the adsorption energies near the linkers and metal oxide cores. The main objective is to optimize the E_{ads} as well as the number of sites per unit volume while keeping the matrix lightweight.

III. ADSORPTION ENHANCEMENT NEAR ORGANIC LINKER

In order to develop better understanding of the calculated adsorption energies we construct a smaller model of MOF-5 fragment with benzene-dicarboxylate and two terminal zinc atoms, 2Zn-BDC (total 18 atoms). With the fully optimized 2Zn-BDC structures, the adsorption energy E_{ads} near benzene sites (i) and (ii) are computed. This much smaller model essentially reproduces the E_{ads} values obtained for MOF-5. However, there is some difference in the E_{ads} values for sites near the oxygen and metal. This could be due to the fact that Zn in 2Zn-BDC is not fully coordinated. Subsequently, E_{ads} is calculated (Table III) with optimized structures of 2*M*-BDC (*M* stands for metals) containing transition metals (Ti, V, Cr, Mn, Fe, Co, Ni, Cu, and Zn) and *p*-block metal Al. It is interesting to note that H_2 adsorption energies near benzene (oriented perpendicular as well as parallel to the benzene plane) are not strongly affected by metal species in the SBU. Sagara *et al.*[25] performed careful investigation of the change in E_{ads} due to charge transfer from the metal to the ligand using $Zn_4O(HCO_2)_5 \cdot BDC \cdot Li$ fragment. This gave results halfway between Li terminated and zinc oxide terminated molecules. However, the charge transfer leads to an increase of E_{ads} values for benzene site by only ~4%. This agrees pretty much with our analysis.

TABLE III. Calculated E_{ads} for H_2 near benzene in the representative model of MOF-5, 2M-BDC (*M*—metal), containing 18 atoms. The zero-point vibrational energies have been ignored.

Metal	E_{ads} near benzene (eV/H_2)	H–H bond length (Å)	Distance of H_2 center from benzene center (Å)
Zn	−0.087	0.768 25	2.735
Cu	−0.090	0.768 45	2.777
Ni	−0.088	0.768 32	2.782
Co	−0.089	0.768 45	2.743
Fe	−0.090	0.768 45	2.742
Mn	−0.087	0.768 35	2.739
Cr	−0.089	0.768 40	2.742
V	−0.093	0.768 80	2.747
Ti	−0.100	0.769 31	2.738
Al	−0.084	0.768 02	2.743

Substitutions of nitrogen in the benzene ring are known to strongly alter the electronic structure of benzene. So next we use $C_4H_4N_2$ (pyrazine) instead of benzene for the organic linker. Hydrogen adsorption energies are calculated for site (v) near the nitrogen oriented perpendicular to the pyrazine-dicarboxylate (PDC) plane and site (vi) at the center oriented perpendicular to the PDC plane [shown as part of a framework in Fig. 5(a)], for 2Zn-PDC, 2Al-PDC, 2Cu-PDC, and PDC-substituted MOF-5. In all cases site (vi) has lower E_{ads} than site (v). E_{ads} for these are −0.159 to −0.164 eV/H_2, except for 2Zn-PDC where E_{ads}=−0.102 eV/H_2. This value is larger than the binding energy of H_2 oriented perpendicular to benzene ring by 80%. Thus the presence of nitrogen in the benzene ring significantly enhances E_{ads}. Mulder *et al.*[28] reported substitutions of F and Br in the BDC linker; however, they found the adsorption energy to decrease. Sagara *et al.*[25] performed calculations with additions of CH_3 and NH_2 to benzene in BDC linker, which resulted in ~30% increase in E_{ads} near the linker. However, addition of these bulky groups may reduce access to the metal oxide core. The presence of nitrogen in the benzene ring does not hinder access to the metal oxide core and therefore might be a better option for further enhancement of H_2 sorption.

Downloaded 01 Sep 2006 to 164.107.79.177. Redistribution subject to AIP license or copyright, see http://jcp.aip.org/jcp/copyright.jsp

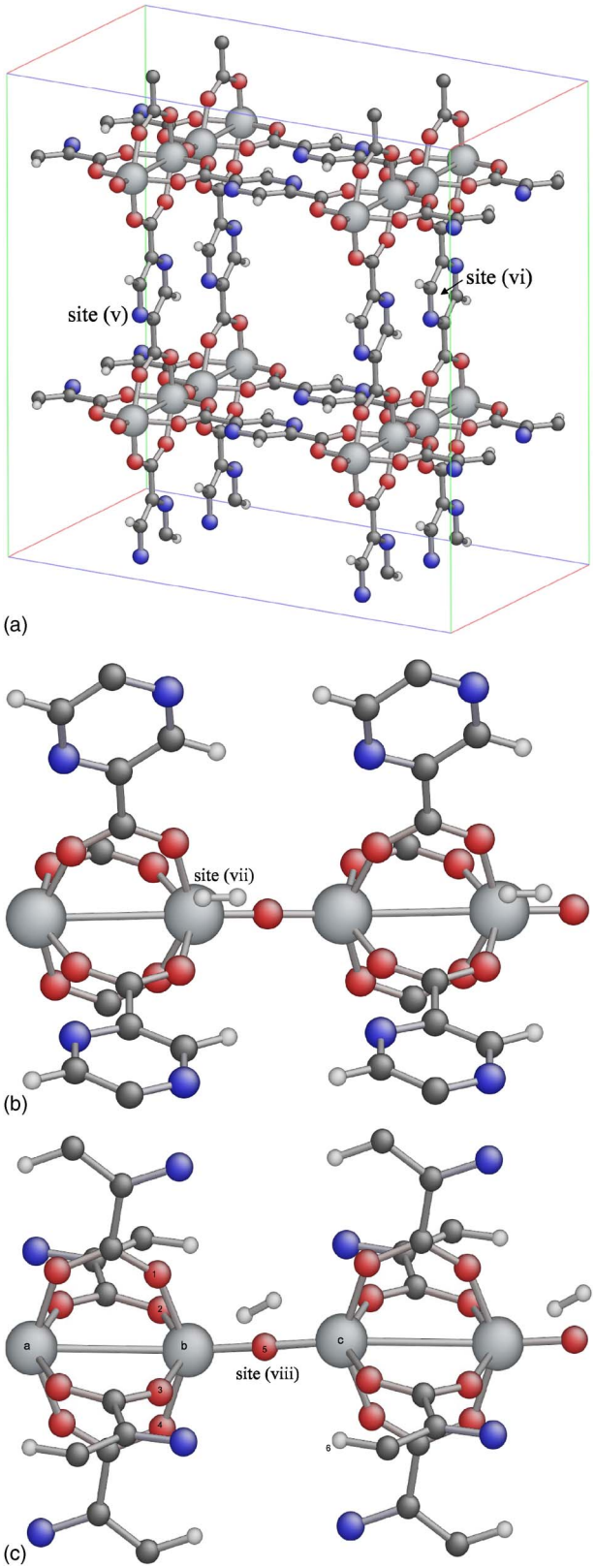

FIG. 5. (a) Equilibrium structure of P-1 (O, red; C, black; H, white; N, blue). (b) H_2 adsorbed near oxygen of pyrazine-dicarboxylate (H_2 center at 2.73 Å from carboxylate oxygen) in P-1. (c) H_2 adsorbed near oxygen ion between two metal cores (H_2 center at 2.77 Å from oxygen) in P-1.

IV. ADSORPTION ENHANCEMENT NEAR METAL OXIDE CORE

It is not clear from the calculations done on MOF-5 whether Zn or O of core is more important in the larger E_{ads} compared to the organic linkers, since O of BDC is quite close to Zn [Fig. 4(b): Zn–O bond length is 1.92 Å, while H_2 is 3.06 and 3.2 Å away from the nearest Zn and O, respectively]. Therefore calculations are done on MOF-5 structure with Zn substituted by transition metals, Cu, Cr, Mn, and Fe, and *p*-block metal Al. However, these yield E_{ads} values comparable to Zn-MOF-5 [for instance, in Al-MOF-5, site (iv), $E_{ads}=-0.163$ eV; site (iii), $E_{ads}=-0.108$ eV; and benzene sites, $E_{ads}=-0.069$ to -0.089 eV]. Spin polarization has been taken into account in these calculations. Our results show that there is little effect of substitution of Al and other metals in the MOF-5 structure. Barbosa *et al.*[60] studied the effect of metal coordination number on the hydrogen adsorption energy in zeolites. It was reported that metals with coordination number 4 tend to have smaller adsorption energy as they are symmetrically surrounded by oxygen which screens the charge of the metal. This could be argued to be the reason for the little change in E_{ads} for MOF-5 with different metals.

In an effort to develop structures with higher H_2 adsorption energies, structures similar to MOF-2 and other network structures[61–63] in which the metal can have a coordination number of 5 are studied. The metal oxide core of MOF-5 accounts for much of the unit cell volume and weight and unfortunately does not provide many useful sites for H_2 adsorption. Another disadvantage of MOF-5 is that much of the pore volume ~ 1 cm^3/g (which is a considerable fraction of the unit cell)[49] is rendered useless. Also, strong adsorption sites are close to each other which makes it difficult for H_2 molecules to freely adhere to these sites. A framework structure having smaller metal oxide cores such as MOF-2 could be a viable alternative to MOF-5. The structure of copper (II) benzoate bridged by pyrazine and –O– is somewhat similar to MOF-2 but has more well-defined open channels. Knowing well from our calculations that E_{ads} is higher near oxygen of the BDC in the case of MOF-5, we propose new framework structures with five-coordinated Al, Cu, and Zn as metal in the SBU (as in MOF-2) and PDC linkers [Fig. 5(a)]. We name these structures with Al, Cu, and Zn in the SBU as P-1, P-2, and P-3 frameworks, respectively. A unit cell of $6.85\times10.67\times10.67$ $Å^3$ with 33 atoms is used for the calculations of P-1, and 35 atoms/unit cell for P-1 but with BDC instead of PDC linkers (hereon called P-1′). We use a $3\times3\times3$ **k**-point mesh. Also strict convergence criteria are used to obtain relaxed structures: relaxation stops when the total energy difference between two consecutive electronic iterations is less than 10^{-6} eV and that of ionic relaxations less than 10^{-5} eV. As shown in Fig. 5(c), the metal (site b)-oxygen (site 5)-metal (site c) bond angle is 180°, whereas the metal (site a)-metal (site b)-oxygen (site 5) bond angle is $\sim$170°. The metal (site b)-oxygen (site 5) bond length is $\sim$1.73 Å while the rest metal-oxygen bond lengths are $\sim$1.94 Å. A small dihedral angle of $\Theta=6.5°-9.2°$ is observed between the benzene plane and carboxylate in these structures.

Volume relaxations are performed to obtain an optimal unit cell size. Following that, adsorption calculations are performed keeping the cell size fixed. With relaxed structures

Downloaded 01 Sep 2006 to 164.107.79.177. Redistribution subject to AIP license or copyright, see http://jcp.aip.org/jcp/copyright.jsp

TABLE IV. Calculated lowest E_{ads} for H_2 in P-1, P-1′, P-2, and P-3 framework structures. The zero-point vibrational energies have been ignored.

Structure	Lowest E_{ads} (eV/H_2)	Site
P-1 (Al)	−0.230	(viii)
P-1′ (Al, but with BDC)	−0.226	(viii)
P-2 (Cu)	−0.291	(viii)
P-3 (Zn)	−0.110	(viii)

for P-1, P-1′, P-2, and P-3, hydrogen adsorption energies are calculated at various sites, such as site (vii) oxygen of the carboxylate [Fig. 5(b)] and site (viii) [Fig. 5(c)]. *Ab initio* molecular dynamics simulations performed for 9 ps, in time steps of 1.5 fs, at $T=300$ K and 400 K show that the framework structures are probably stable at these temperatures. The amplitude of atomic motion in these structures appears to be significant though. For example, the metal atom at site b appears to move during *ab initio* MD at $T=400$ K with amplitude of ~0.5 Å. For H_2 placed in sites (vii) and (viii) the nearest atom from the center of H_2 molecule is oxygen, ~2.74 Å. Table IV shows the E_{ads} results. Calculations are also done with Cl substitution of H [site 6 in Fig. 5(c)] in pyrazine and the E_{ads} values are nearly identical with previous values in Sec. III (−0.16 eV/H_2). These P-series structures have very high E_{ads} values compared to MOF-5 and are worthy of further theoretical and experimental investigations.

V. SUMMARY

DFT-LDA calculations are performed to predict the elastic constants and band gap for Zn-based MOF-5. The bulk modulus calculations are verified by using a simple Hookean spring model. We predict *xy* shear to be the most vulnerable deformation mode in MOF-5. Detailed calculations are done to find sites of low E_{ads} in MOF-5. The sites near benzene and near oxygen of carboxylate are found to be probable sites for H_2 physisorption. E_{ads}'s in MOF-5 fall short of the desired value of −200 meV/H_2 for room-temperature storage, especially since DFT-LDA calculations tend to overestimate dispersive interactions,[40] and zero-point vibrational energies of the physisorbed states have been neglected.

Various possibilities of enhancing the adsorption energy near the organic linker and metal core are studied, specifically the presence of nitrogen in benzene and five-coordinated metal cation in SBU. Electrophilic substitutions of OH and Cl to the benzene do not lead to an increase in E_{ads}. E_{ads} near the benzene sites is not highly sensitive to metal species in the metal oxide core, but can be significantly enhanced by as much as 80% after nitrogen substitution in the benzene ring. E_{ads} near the metal core can be enhanced greatly by using pentacoordinated metals (aluminum or copper) in the SBU that break the high symmetry of four-coordinated metals in MOF-5. Physisorption energies are calculated at various sites in new framework structures P-1, P-1′, P-2, and P-3. The calculated DFT-LDA values of adsorption energies (near the metal oxide core as well as the linkers) are exceptionally higher than those reported for existing frameworks. For ease of checking, the input and output files of our calculations are put at a publicly accessible website.[64] The results of this work may guide future rational design of MOF materials with improved hydrogen adsorption capacity at room temperature.

ACKNOWLEDGMENTS

We acknowledge support by Honda R&D Co., Ltd., Ohio Supercomputer Center, and the OSU Transportation Research Endowment Program. We also thank Joshua Fujiwara and Karl Johnson for discussions.

[1] O. M. Yaghi, H. L. Li, C. Davis, D. Richardson, and T. L. Groy, Acc. Chem. Res. **31**, 474 (1998).
[2] M. Eddaoudi, D. B. Moler, H. L. Li, B. L. Chen, T. M. Reineke, M. O'Keeffe, and O. M. Yaghi, Acc. Chem. Res. **34**, 319 (2001).
[3] B. Moulton and M. J. Zaworotko, Chem. Rev. (Washington, D.C.) **101**, 1629 (2001).
[4] C. Janiak, Dalton Trans. **2003**, 2781 (2003).
[5] M. J. Rosseinsky, Microporous Mesoporous Mater. **73**, 15 (2004).
[6] H. K. Chae, D. Y. Siberio-Perez, J. Kim, Y. Go, M. Eddaoudi, A. J. Matzger, M. O'Keeffe, and O. M. Yaghi, Nature (London) **427**, 523 (2004).
[7] L. Schlapbach and A. Zuttel, Nature (London) **414**, 353 (2001).
[8] L. Schlapbach, MRS Bull. **27**, 675 (2002).
[9] S. M. Aceves, G. D. Berry, and G. D. Rambach, Int. J. Hydrogen Energy **23**, 583 (1998).
[10] A. M. Seayad and D. M. Antonelli, Adv. Mater. (Weinheim, Ger.) **16**, 765 (2004).
[11] A. Zuttel, P. Wenger, S. Rentsch, P. Sudan, P. Mauron, and C. Emmenegger, J. Power Sources **118**, 1 (2003).
[12] A. Zuttel, P. Sudan, P. Mauron, T. Kiyobayashi, C. Emmenegger, and L. Schlapbach, Int. J. Hydrogen Energy **27**, 203 (2002).
[13] J. Li, T. Furuta, H. Goto, T. Ohashi, Y. Fujiwara, and S. Yip, J. Chem. Phys. **119**, 2376 (2003).
[14] J. Li and S. Yip, J. Chem. Phys. **120**, 9430 (2004).
[15] M. Hirscher, M. Becher, M. Haluska, F. von Zeppelin, X. H. Chen, U. Dettlaff-Weglikowska, and S. Roth, J. Alloys Compd. **356**, 433 (2003).
[16] S. H. Jhi and Y. K. Kwon, Phys. Rev. B **69**, 245407 (2004).
[17] H. W. Langmi, A. Walton, M. M. Al-Mamouri, S. R. Johnson, D. Book, J. D. Speight, P. P. Edwards, I. Gameson, P. A. Anderson, and I. R. Harris, J. Alloys Compd. **356**, 710 (2003).
[18] A. W. C. van den Berg, S. T. Bromley, and J. C. Jansen, Microporous Mesoporous Mater. **78**, 63 (2005).
[19] H. Li, M. Eddaoudi, M. O'Keeffe, and O. M. Yaghi, Nature (London) **402**, 276 (1999).
[20] W. Kohn, A. D. Becke, and R. G. Parr, J. Phys. Chem. **100**, 12974 (1996).
[21] D. M. Ceperley and B. J. Alder, Phys. Rev. Lett. **45**, 566 (1980).
[22] J. P. Perdew and A. Zunger, Phys. Rev. B **23**, 5048 (1981).
[23] J. L. C. Rowsell, A. R. Millward, K. S. Park, and O. M. Yaghi, J. Am. Chem. Soc. **126**, 5666 (2004).
[24] T. Sagara, J. Klassen, and E. Ganz, J. Chem. Phys. **121**, 12543 (2004).
[25] T. Sagara, J. Klassen, J. Ortony, and E. Ganz, J. Chem. Phys. **123**, 014701 (2005).
[26] G. Garberoglio, A. I. Skoulidas, and J. K. Johnson, J. Phys. Chem. B **109**, 13094 (2005).
[27] T. Mueller and G. Ceder, J. Phys. Chem. B **109**, 17974 (2005).
[28] F. M. Mulder, T. J. Dingemans, M. Wagemaker, and G. J. Kearley, Chem. Phys. **317**, 113 (2005).
[29] T. Sagara, J. Ortony, and E. Ganz, J. Chem. Phys. **123**, 214707 (2005).
[30] T. Yildirim and M. R. Hartman, Phys. Rev. Lett. **95**, 215504 (2005).
[31] J. P. Perdew and Y. Wang, Phys. Rev. B **45**, 13244 (1992).
[32] J. P. Perdew, K. Burke, and M. Ernzerhof, Phys. Rev. Lett. **77**, 3865 (1996).
[33] I. Cabria, M. J. Lopez, and J. A. Alonso, J. Chem. Phys. **123**, 204721 (2005).
[34] H. Rydberg, N. Jacobson, P. Hyldgaard, S. I. Simak, B. I. Lundqvist, and D. C. Langreth, Surf. Sci. **532**, 606 (2003).
[35] K. Tada, S. Furuya, and K. Watanabe, Phys. Rev. B **63**, 155405 (2001).
[36] J. S. Arellano, L. M. Molina, A. Rubio, and J. A. Alonso, J. Chem. Phys.

Downloaded 01 Sep 2006 to 164.107.79.177. Redistribution subject to AIP license or copyright, see http://jcp.aip.org/jcp/copyright.jsp

112, 8114 (2000).
[37] J. S. Arellano, L. M. Molina, A. Rubio, M. J. Lopez, and J. A. Alonso, J. Chem. Phys. **117**, 2281 (2002).
[38] I. Cabria, M. J. Lopez, and J. A. Alonso, Comput. Mater. Sci. **35**, 238 (2006).
[39] Y. Okamoto and Y. Miyamoto, J. Phys. Chem. B **105**, 3470 (2001).
[40] A. J. Du and S. C. Smith, Nanotechnology **16**, 2118 (2005).
[41] X. Wu, M. C. Vargas, S. Nayak, V. Lotrich, and G. Scoles, J. Chem. Phys. **115**, 8748 (2001).
[42] A. Dailly, J. J. Vajo, and C. C. Ahn, J. Phys. Chem. B **110**, 1099 (2006).
[43] I. Efremenko and M. Sheintuch, Langmuir **21**, 6282 (2005).
[44] P. E. Blochl, Phys. Rev. B **50**, 17953 (1994).
[45] G. Kresse and J. Furthmuller, Phys. Rev. B **54**, 11169 (1996).
[46] G. Kresse and D. Joubert, Phys. Rev. B **59**, 1758 (1999).
[47] H. J. Monkhorst and J. D. Pack, Phys. Rev. B **13**, 5188 (1976).
[48] W. H. Press, B. P. Flannery, S. A. Teukolsky, and W. T. Vetterling, *Numerical Recipes in C: The Art of Scientific Computing* (Cambridge University Press, Cambridge, 1992).
[49] O. M. Yaghi, M. O'Keeffe, N. W. Ockwig, H. K. Chae, M. Eddaoudi, and J. Kim, Nature (London) **423**, 705 (2003).
[50] N. W. Ockwig, O. Delgado-Friedrichs, M. O'Keeffe, and O. M. Yaghi, Acc. Chem. Res. **38**, 176 (2005).
[51] J. H. Wang, J. Li, S. Yip, S. Phillpot, and D. Wolf, Phys. Rev. B **52**, 12627 (1995).
[52] J. Li, K. J. Van Vliet, T. Zhu, S. Yip, and S. Suresh, Nature (London) **418**, 307 (2002).
[53] P. N. Keating, Phys. Rev. **145**, 637 (1966).
[54] M. Eddaoudi, J. Kim, D. Vodak, A. Sudik, J. Wachter, M. O'Keeffe, and O. M. Yaghi, Proc. Natl. Acad. Sci. U.S.A. **99**, 4900 (2002).
[55] M. E. Braun, C. D. Steffek, J. Kim, P. G. Rasmussen, and O. M. Yaghi, Chem. Commun. (Cambridge) **2001**, 2532.
[56] S. Bordiga, C. Lamberti, G. Ricchiardi, L. Regli, F. Bonino, A. Damin, K. P. Lillerud, M. Bjorgen, and A. Zecchina, Chem. Commun. (Cambridge) **2004**, 2300.
[57] Z. H. Levine and D. C. Allan, Phys. Rev. Lett. **63**, 1719 (1989).
[58] N. L. Rosi, J. Eckert, M. Eddaoudi, D. T. Vodak, J. Kim, M. O'Keeffe, and O. M. Yaghi, Science **300**, 1127 (2003).
[59] K. A. Williams, B. K. Pradhan, P. C. Eklund, M. K. Kostov, and M. W. Cole, Phys. Rev. Lett. **88**, 165502 (2002).
[60] L. Barbosa, G. M. Zhidomirov, and R. A. van Santen, Catal. Lett. **77**, 55 (2001).
[61] R. Nukada, W. Mori, S. Takamizawa, M. Mikuriya, M. Handa, and H. Naono, Chem. Lett. 367 (1999).
[62] G. J. Gainsford, T. Kemmitt, and N. B. Milestone, Inorg. Chem. **34**, 5244 (1995).
[63] V. Niel, J. M. Martinez-Agudo, M. C. Munoz, A. B. Gaspar, and J. A. Real, Inorg. Chem. **40**, 3838 (2001).
[64] http://alum.mit.edu/www/liju99/Papers/06/Samanta06a

Downloaded 01 Sep 2006 to 164.107.79.177. Redistribution subject to AIP license or copyright, see http://jcp.aip.org/jcp/copyright.jsp